

UVM ScholarWorks

Impact of an Extreme Storm Event on River Corridor Bank Erosion and Phosphorus Mobilization in a Mountainous Watershed in the Northeastern United States

Item Type	article;article
Authors	Ross, Donald S.;Wemple, Beverley C.;Willson, Lindsay J.;Balling, Courtney M.;Underwood, Kristen L.;Hamshaw, Scott D.
Citation	Ross DS, Wemple BC, Willson LJ, Balling CM, Underwood KL, Hamshaw SD. Impact of an extreme storm event on river corridor bank erosion and phosphorus mobilization in a mountainous watershed in the Northeastern United States. Journal of Geophysical Research: Biogeosciences. 2019 Jan 1;124(1):18-32.
DOI	10.1029/2018JG004497
Rights	©2018. American Geophysical Union. All Rights Reserved.; http://rightsstatements.org/vocab/InC/1.0/
Download date	2026-05-13 10:46:48
Link to Item	https://hdl.handle.net/20.500.14849/342



RESEARCH ARTICLE

10.1029/2018JG004497

Special Section:

Extreme Climate Event Impacts on Aquatic Biogeochemical Cycles and Fluxes

Key Points:

- Extreme event-induced stream bank movement along six eroding sites generated sediment loads equivalent to average annual watershed exports
- Phosphorus loads were also high, but short-term phosphorus release may be limited because of low bioavailability in the eroded sediment
- Stripping of riparian buffers and lateral bank retreat into actively managed agricultural fields may enhance future phosphorus losses

Supporting Information:

- Supporting Information S1
- Data Set S1

Correspondence to:

D. S. Ross, dross@uvm.edu

Citation:

Ross, D. S., Wemple, B. C., Willson, L. J., Balling, C. M., Underwood, K. L., & Hamshaw, S. D. (2019). Impact of an extreme storm event on river corridor bank erosion and phosphorus mobilization in a mountainous watershed in the Northeastern United States. *Journal of Geophysical Research: Biogeosciences*, 124, 18–32. <https://doi.org/10.1029/2018JG004497>

Received 17 MAR 2018

Accepted 26 NOV 2018

Accepted article online 6 DEC 2018

Published online 4 JAN 2019

Author Contributions:

Conceptualization: Donald S. Ross, Beverley C. Wemple, Kristen L. Underwood




Data curation: Donald S. Ross

Formal analysis: Donald S. Ross, Beverley C. Wemple, Lindsay J. Willson, Courtney M. Balling, Kristen L. Underwood, Scott D. Hamshaw

Investigation: Donald S. Ross, Beverley C. Wemple, Lindsay J. Willson, Courtney M. Balling (continued)

©2018. American Geophysical Union. All Rights Reserved.

Impact of an Extreme Storm Event on River Corridor Bank Erosion and Phosphorus Mobilization in a Mountainous Watershed in the Northeastern United States

Donald S. Ross¹ , Beverley C. Wemple², Lindsay J. Willson^{2,3}, Courtney M. Balling^{1,4}, Kristen L. Underwood⁵ , and Scott D. Hamshaw^{5,6} 

¹Department of Plant and Soil Science, University of Vermont, Burlington, VT, USA, ²Geography Department, University of Vermont, Burlington, VT, USA, ³Now at School of Forestry and Environmental Studies, Yale University, New Haven, CT, USA, ⁴Now at Department of Crop and Soil Sciences, University of Georgia, Athens, GA, USA, ⁵Civil and Environmental Engineering, University of Vermont, Burlington, VT, USA, ⁶Vermont EPSCoR, University of Vermont, Burlington, VT, USA

Abstract Movement of sediment, and associated phosphorus, from stream banks to freshwater lakes is predicted to increase with greater frequency of extreme precipitation events. This higher phosphorus load may accelerate harmful algal blooms in affected water bodies, such as Lake Champlain in Vermont, New York, and Québec. In the Mad River, a subwatershed in central Vermont's Lake Champlain Basin, extreme flooding from Tropical Storm Irene in 2011 caused extensive erosion. We measured stream channel change along the main stem between 2008 and 2011 by digitizing available prestorm and poststorm aerial imagery. Soils were sampled post Irene at six active stream erosion sites, using an experimental design to measure differences in soil texture and phosphorus both with depth (90 cm) and distance from the stream. In addition to total phosphorus (TP), we determined bioavailable (soil test) phosphorus (STP) and the degree of phosphorus saturation (DPS). The six sites represented a 0.87-km length of stream bank that contributed an estimated 17.6×10^3 Mg of sediment and 15.8 Mg of TP, roughly the same as average annual watershed export estimates. At four sites, the STP and DPS were low and suggested little potential for short-term phosphorus release. At two agricultural sites where the lateral extent of erosion was high, imagery showed a clear loss of well-established riparian buffer. Present-day near-stream soils were elevated in STP and DPS. An increase in these extreme events will clearly increase sediment loads. There will also be increasing concentration of sediment phosphorus if stream banks continue to erode into actively managed agricultural fields.

Plain Language Summary Extreme precipitation events can cause streams to swell above their banks and erode near-stream soil. Because stream bank soils contain phosphorus, increased erosion can increase the transport of phosphorus into lakes, leading to harmful algal blooms. Our study occurred in central Vermont along the Mad River, which flows into Lake Champlain. Tropical Storm Irene delivered a record amount of rainfall to much of Vermont. Soils were already wet and streams quickly flooded, causing drastic stream channel changes. We used aerial photography to measure the change in stream channel and calculated the amount of soil lost. We also sampled soil at six erosion sites, measuring various forms of phosphorus. These measurements suggest that one extreme event delivered as much sediment and phosphorus into the stream as is normally exported over an entire year. Bioavailable phosphorus was low in most soil samples. However, high erosion along two agricultural fields removed large trees that formed a buffer with the stream and pushed present-day stream banks well back into the farmland. These soils had elevated amounts of bioavailable phosphorus and would likely contribute more toward downstream eutrophication if erosion continues. The effect of this one extreme event will continue to be felt for years to come.

1. Introduction

A number of regions of the world, including the northeastern United States, have experienced increases in precipitation in recent decades. This trend is forecast to continue (Intergovernmental Panel on Climate Change, 2013), along with an increase in extreme precipitation events, such as those delivered by tropical cyclones or their remnants (Horton & Liu, 2014). These events have the potential to drastically alter both stream geomorphology and ecology (Death et al., 2015; Naylor et al., 2017), and riparian zone biogeochemical behavior (Vidon et al., 2017). Event-induced increases in stream bank erosion and sediment export are

M. Balling, Kristen L. Underwood, Scott D. Hamshaw

Methodology: Donald S. Ross, Beverley C. Wemple, Kristen L. Underwood, Scott D. Hamshaw

Resources: Donald S. Ross, Beverley C. Wemple

Supervision: Donald S. Ross, Beverley C. Wemple, Kristen L. Underwood

Validation: Beverley C. Wemple, Scott D. Hamshaw

Visualization: Donald S. Ross, Beverley C. Wemple, Lindsay J. Willson, Kristen L. Underwood

Writing - original draft: Donald S. Ross, Kristen L. Underwood

Writing - review & editing: Donald S. Ross, Beverley C. Wemple, Lindsay J. Willson, Courtney M. Balling, Kristen L. Underwood, Scott D. Hamshaw

associated with the high stream power resulting from extreme events (Magilligan et al., 2015). This increased erosion, in turn, will increase sediment-associated phosphorus (P) loading to streams and may contribute to eutrophication and harmful algal blooms in sensitive, downstream water bodies (Anderson et al., 2002; Carpenter et al., 1998; Vidon et al., 2018).

Extreme events are well recognized for the role they play in sediment production and export through river basins (Gonzalez-Hidalgo et al., 2010). Climate change-induced changes in precipitation intensity and frequency are expected to alter erosion rates in diverse settings (Nearing et al., 2004). Within the northeastern United States, studies of the impact of extreme precipitation events have shown they have the potential to accelerate erosion and export more sediment load in a single event than the long-term annual average, as observed during Tropical Storm Irene in the Connecticut River (Yellen et al., 2014). A number of studies have attempted to model the impact of changing climate regimes, particularly the occurrence of extreme storm events on sediment production and yield, identifying stream bank erosion as a key contributor to sediment fluxes under the type of extreme events expected in the future (Bussi et al., 2014; Stryker et al., 2018).

Stream bank erosion can be a measureable source of P loading, as has been documented in a number of agricultural regions (Fox et al., 2016). Estimates of the magnitude of this contribution vary among watersheds and locations. For example, in a Danish lowland river, Kronvang et al. (2012) found that stream banks contributed 17–29% of the annual total phosphorus (TP) export. Sekely et al. (2002) estimated that 7–10% of the annual TP load from the Blue Earth River in Minnesota came from stream bank slumping. Estimates from other parts of the United States have been within these ranges (Fox et al., 2016). In the Lake Champlain Basin of Vermont, stream bank inputs to annual TP losses have been estimated at 36% in the northern Missisquoi River watershed (Langendoen et al., 2012) and 6–30% in small central (less agricultural) tributaries (Ishee et al., 2015). Dewolfe et al. (2004) found on average that 25% of annual TP losses came from stream bank erosion in four Basin streams but with high variability along different reaches (2–92%). Although these studies reveal both spatial and temporal variability, stream banks can contribute over one third of the annual TP export.

Riparian buffers help to attenuate and filter overland flow and stabilize stream bank soils, thereby reducing erosion and transport of sediment and associated TP (Osborne & Kovacic, 1993). Presence of aboveground biomass (e.g., tree trunks and branches) in the floodplain increases hydraulic resistance, slowing overland flow velocities that attenuate and trap sediment transported by flood flows. The dense root systems of woody vegetation increase soil shear strength and stability relative to unvegetated soils (Abernethy & Rutherford, 2000), although there is a range among species in root morphology and resulting effectiveness (Merritt, 2013). Miller et al. (2014), working in an Oklahoma watershed, measured about 3 times greater stream bank recession rates and greater TP losses from sites without riparian protection. Zaines et al. (2008) showed much lower erosional and TP losses from stream bank sites with forested or grass riparian buffers compared to sites with no buffer in Iowa catchments. Extreme events can reduce the effectiveness of riparian buffers, if excessive channel widening leads to reduced buffer widths or if a sudden channel avulsion bypasses the riparian buffer altogether. These buffer-compromised sites, in turn, are susceptible to increased erosion during future events.

On 28 August 2011, Tropical Storm Irene delivered up to 20 cm of rain to parts of Vermont, causing extensive flooding damage (Anderson et al., 2017; Buraas et al., 2014). Portions of Vermont experienced 12-hr rainfall amounts at a >500-year recurrence interval (RI; Anderson et al., 2017), and a number of streams experienced record flows with RI flooding of 300–1,000 years (Magilligan et al., 2015). Rainfall intensity was greatest along the spine of the southern Green Mountains resulting in extensive landslides and mass wasting (Dethier et al., 2016). Flooding effects, chiefly channel avulsion and coarse sediment deposition in floodplains, were more pronounced and documented in the Connecticut River watershed of southeastern Vermont (Dethier et al., 2016; Magilligan et al., 2015; Yellen et al., 2016). However, the central subwatersheds of the Lake Champlain basin also experienced >100-year RI flooding including the north flowing Mad River at >200 RI peak flow (Olson, 2014) and the upper Winooski River basin (Olson, 2015). The intensity of the flooding was not only exacerbated by high antecedent soil moisture (Yellen et al., 2016) but also somewhat dampened by the relatively short period (<12 hr) of intense precipitation (Magilligan et al., 2015).

The Mad River is a tributary to the Winooski River, which drains to Lake Champlain, a lake that has experienced increasing frequency of harmful algal blooms in recent years (Isles et al., 2015), and is the subject of restoration plans for P reduction (Smeltzer et al., 2012). Working at primarily agricultural sites along the

main stem of the Mad River, we used a combination of aerial image analysis, elevation data from unmanned aircraft surveys (UAS; Hamshaw et al., 2017), and soil sampling to estimate the amount of stream bank sediment and associated TP lost to the stream from <1 km of stream bank length during the extreme flooding caused by Tropical Storm Irene. These six sites were chosen because of their stream bank erosion potential. Our study was designed specifically to measure change only at these sites along the floodplain of the main stem to demonstrate the disproportionately important role of at-risk eroding stream banks to material loads during extreme events. To do this, we compare the site-specific estimates for this event with separate estimates of erosion along the main stem and estimates of watershed export of both suspended sediment and TP.

2. Materials and Methods

2.1. Mad River Watershed

The main stem of the Mad River (Figure 1) runs 35 km north from Granville and Warren to its junction with the Winooski River in Moretown, Vermont. The 373-km² watershed comprises the eastern slopes of the main ridge of the Green Mountains (highest elevation 1,232 m) and the western slopes of a secondary ridge (~850-m elevation). Most (86%) of the watershed is forested with 5% in agriculture, 8% developed, and 1% other (Troy et al., 2007). Because of the steep nature of the watershed, much of the agricultural and developed land lies along the valley floor, close to the main stem and major tributaries of the Mad River. Within a typical year, a majority of the runoff occurs between ice-out and late spring (Shanley & Denner, 1999). Floods often result from snow melt or rain-on-snow events but can also be associated with convective storms or tropical systems in summer or fall. A United States Geological Survey (USGS) gauge (04288000) has been monitoring discharge near the confluence with the Winooski River since 1928. A 2-year RI discharge is estimated as 163 m³/s (Olson, 2014). The peak discharge of 685 m³/s on 28 September 2011 during Irene was 1.05 times higher than the previous record from 3 November 1927 (Olson, 2014). In addition to the stream bank erosion described below, this storm caused considerable overbank flow and floodplain sediment deposition, along with extensive structural damage to bridges (Anderson et al., 2017).

2.2. Sites and Soil Sampling

In 2013, six study sites were selected along the Mad River main stem where the aerial imaging, described under section 2.4, showed historic channel movement and where landowner permission could be obtained. Soils at all sites had alluvial parent material and were mapped as Inceptisols in the United States Department of Agriculture (USDA) Natural Resources Conservation Service (NRCS) taxonomic system, namely, Fluventic Dystrudepts and Fluvaquentic Endoaquepts (Soil Survey Staff, 2017a). To examine differences in soil properties from the stream edge into the adjacent land use, two lateral transects, 4 m apart, were established at each site perpendicular to the stream. Transects were located to minimize sampling of recent flood deposits. Based on imagery taken 4 weeks post Irene (Figures 2 and S1), and field observations, Irene sediment deposition at our sampling sites appeared minor. Site E did have some evidence of a recently buried soil horizon at a depth of about 15 cm. Samples were taken at three points along each transect: 1 m back from the top of the stream bank edge, midway through the riparian buffer (if present and >3 m wide), and 10 m into the field (Figure S1). To capture vertical variability, soil samples were taken with a 5-cm bucket auger to a depth of 90 cm, when possible, in four increments: 0–15, 15–30, 30–60, and 60–90 cm. Data from the two transect points were averaged. A few points had gravel or larger coarse fragments preventing sampling below 60 cm. To characterize the spatial variability in soil properties, six additional 0- to 15-cm samples were taken from each location (stream bank edge, buffer, and field) 10 m perpendicular from each transect, or longitudinally along the stream (Figure S1). Two to four separate samples of the stream bank itself were taken at each site 0–15 cm into the bank at 1-m spacing down the bank slope. At Sites C and E, additional depth samples were taken at one of the stream bank edge points to 150 and 120 cm, respectively. In order to convert soil volume measurements to mass, bulk density samples were taken using a 9.8-cm hammer-driven bulk density corer in the 0- to 15-cm depth of the main transect points and along the stream banks.

The land use/land cover at the six sites presented here included hay fields associated with active dairy/beef farms, small-scale vegetable production, and forest (Table 1). The riparian vegetated buffer at two sites (A and B) was narrow (<3 m) unmown hay. At two other sites (C and D), the buffer was dominated by *Fallopia japonica* (Japanese knotweed) that anecdotally was reported to spread widely after Irene.

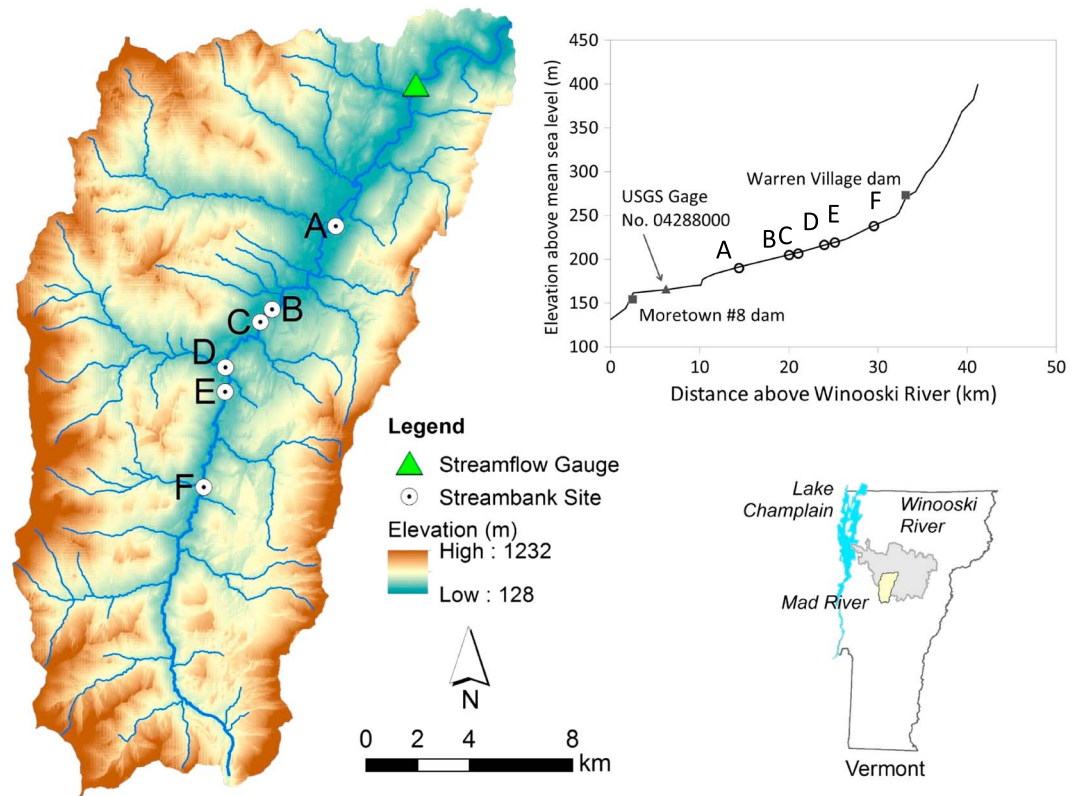


Figure 1. Map of the Mad River Watershed showing the stream network and study sites.

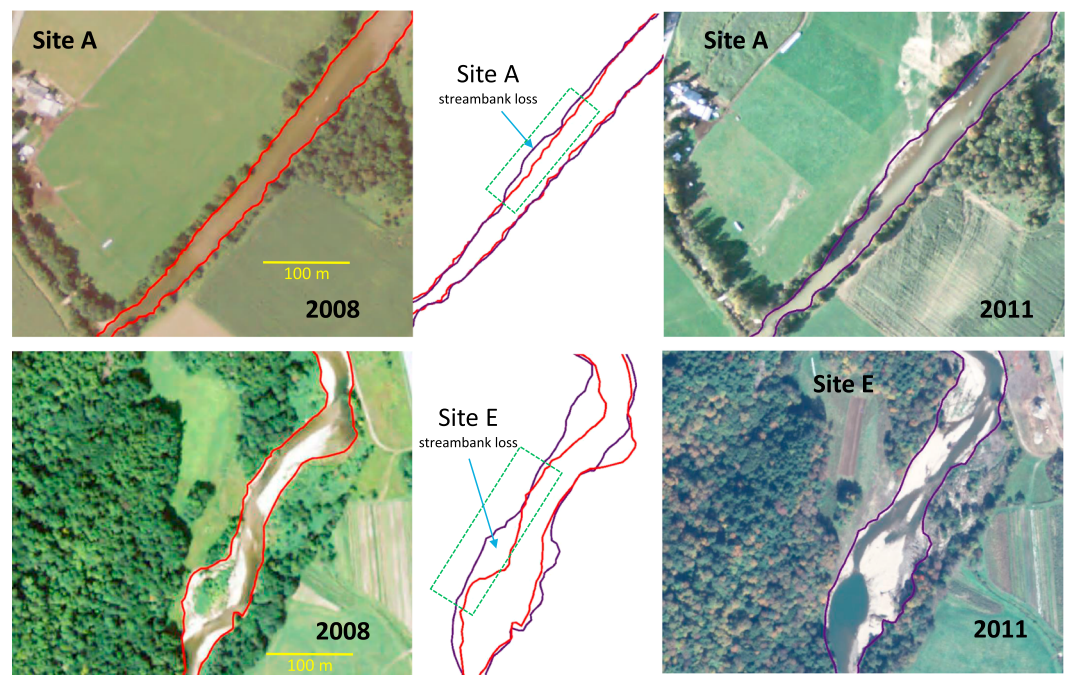


Figure 2. Images of two of the erosion sites (left) before and (right) after (right) Tropical Storm Irene. Digitized stream bank lines are overlapped in the center image to show areas of erosion (red = 2008; blue = 2011). The green rectangle outlines the area of stream bank erosion measurement. See Figure S2 for the remaining sites.

Table 1
Site Characteristics at the Time of Sampling (June–July 2013)

Site	Field vegetation	Buffer width (m)	Buffer vegetation
A	Hay	2.5	Unmown hay
B	Hay	1.5	Unmown hay
C	Hay	23	<i>Fallopia japonica</i>
D	Hay	10	<i>Fallopia japonica</i>
E	Potato	35	Conservation planting ^a
F	Riverine forest ^b	15	Riverine forest

^aNative tree saplings planted in 2013. ^bSugar maple-ostrich fern riverine forest with some open turf grass.

2.3. Laboratory Analyses

All 232 soil samples were air dried and sieved to <2 mm before further analyses. Three forms of soil P were determined: an estimate of TP, the degree of phosphorus saturation (DPS) and a measurement of bioavailable or soil test P (STP). For the first two procedures, subsamples of <2-mm soil were ground to pass through a 0.5-mm sieve before weighing for analysis. TP, the primary measurement used in water quality studies, was estimated by nitric acid microwave-assisted digestion and inductively coupled plasma optical emission spectroscopy using United States Environmental Protection Agency Method 3051 (United States Environmental Protection Agency, 2007). This is a standard method but may give results slightly lower than the true total because of incomplete digestion of

occluded P minerals (Leytem & Kpombekou-A, 2009). The DPS, used to predict the potential to sorb or release soluble P, was determined on 118 of the samples (all stream bank edge but only the 0- to 15-cm main transect samples for the other locations) using the acid ammonium oxalate procedure (Courchesne & Turmel, 2007). This method is intended for noncalcareous soils and extracts the less crystalline forms of Fe and Al that can precipitate added P. The % DPS was calculated using the molar ratio of P to half the sum of Fe plus Al. Prior research with Vermont stream corridor soils found a DPS of <20% in locations with no known history of P additions (Ishee et al., 2015). For an estimate of bioavailable P, the Modified Morgans soil test procedure (pH 4.8 ammonium acetate, 1.25-M acetate) was used (Wolf & Beegle, 2011). Magdoff et al. (1999) found that this extraction, which removes much less P than F-based extractants such as Bray and Mehlich-3, was reasonably well correlated with weak-salt extractable (soluble) P and, as such, is a good indicator of immediately bioavailable P.

Organic matter was determined by weight loss on ignition for 2 hr at 375 °C in a forced air oven, adjusted for an established relationship from samples with known carbon content (Schulte & Hoskins, 2011). Particle size was determined on the near-stream bank depth samples using the hydrometer method after dispersion with sodium hexametaphosphate (Day, 1965). Bulk density cores were dried overnight at 105 °C and sieved to <2 mm, and soil and coarse fragments weighed separately. The volume of the coarse fragments, if present, was calculated assuming a density of 2.65 Mg/m³, and both the volume and weight were subtracted from the final calculation of soil bulk density.

2.4. Measurement of Channel Change and Soil Loss

Aerial imagery from 21 August 2008 (pre-Irene) and 26 September 2011 (post-Irene) was obtained from the National Agriculture Imagery Program (NAIP) and used to digitize channel margins for analysis of areal change. NAIP imagery is acquired at 1-m ground sample distance and has a nominal horizontal accuracy of ±6 m on photo-identifiable ground control points (USDA Farm Service Agency NAIP Imagery, <https://www.fsa.usda.gov/programs-and-services/aerial-photography/imagery-programs/naip-imagery/>, last accessed March 2018). To assess horizontal accuracy in registration of the photo sets used for this study, we identified and digitized 19 control points (building rooftops and road intersections) common on the three orthophoto sets for each year (2008 and 2011). The ArcGIS v. 10.5 (Environmental Systems Research Institute, 2017) NEAR function was used to measure distance between control points across photo years and assess photo offsets, yielding an estimated horizontal error of 2.38 m with a range between 0.90 to 4.54 m. We used this horizontal error estimate to quantify likely error associated with photo registration and manual digitizing, though we acknowledge that quantifying error associated with manual digitizing is challenging. Using the imagery as a visual guide, we digitized the stream margin for each photo year. The areal change along the six sampling sites was measured by creating a polygon of the two stream bank locations (2008 and 2011) bounded by the extent of the field edge along the stream (e.g., Figure S2). An overlay analysis using the ArcGIS UNION function yielded areal change estimates. This approach to change detection assumes a common river stage across the two photo sets such that visual interpretation of the channel margin is not affected by water surface elevation. River stage at the USGS gauge (Figure 1) during the daylight hours was 0.951 and 0.942 m, respectively, for the two photo dates (USGS National Water Information System, <https://waterdata.usgs.gov/usa/nwis/uv?04288000>, last accessed March 2018). The small difference in river stage (9 mm) across these two image dates would have minimal impact on the relative channel delineation.

Table 2
Soil Characteristics at the Near-Stream Sampling Points Averaged Over 0- to 90-cm Depth

Site	Sand (g/kg)		Silt (g/kg)		Clay (g/kg)		Organic matter (g/kg)		Texture ^a
	Mean	SE	Mean	SE	Mean	SE	Mean	SE	
A	704	24.1	228	22.1	69	3.3	23.1	3.1	Sandy loam
B	641	29.1	305	25.0	54	4.7	26.9	3.3	Sandy loam
C	754	7.9	187	9.9	59	4.6	21.2	2.3	Sandy loam
D	699	23.8	242	22.6	59	2.8	25.3	2.8	Sandy loam
E	780	20.4	174	19.3	46	1.9	10.1	0.9	Loamy sand
F	838	15.5	113	13.8	49	3.2	16.4	2.7	Loamy sand

Note. SE = standard error of the mean; USDA = United States Department of Agriculture.
^aUSDA classification.

To assess the vertical extent of channel change, bank heights at each transect point were measured manually in 2013 and from an UAS in 2016 (Hamshaw et al., 2017), with the exception of Site F, which was outside the UAS survey area. Since measurements from the two dates corresponded well at the transect locations, the 2016 UAS survey data were used to generate an average bank height for the length of the field edge. The manually measured 2013 bank height was used as an average for Site F. Because no bank height measurements were available pre-Irene, we assumed the ground surface elevation of the erosion feature was constant at any given cross section. An estimate of bank height variance was derived by calculating the 95% confidence interval (CI) of six bank heights from evenly spaced cross sections along each study site. The average CI from Sites A–E was used for Site F. The UAS elevation data had a median error of 0.11 m (Hamshaw et al., 2017).

Volume of soil lost between 2008 and 2011 was calculated as the product of the surface area estimates described above, and the average bank height along the length of field edge. A corresponding mass of soil loss was calculated using the measured bulk density values. Error in this calculation was estimated using the CI for the bulk density readings. We also calculated silt- and clay-sized particle loss by using the texture analyses in Table 2. To determine TP loss, the average TP to the depth of the stream bank was calculated using data for the near-stream transect points. For depths below 90 cm, the TP concentration was assumed to be the same as in the 60- to 90-cm samples. To estimate the error associated with TP concentration, we used the difference between profile TP values from the two near-stream transect points.

For this study, we assumed that the entire difference in stream bank location between 2008 and 2011 was caused by Tropical Storm Irene and that the extent of scouring, vegetation loss, and sediment deposition evident in post-Irene imagery can largely be explained by that event (Figures 2 and S2). Streamflow gauging records from USGS show that no other storm events exceeding the 2-year RI of 163 m³/s (Olson, 2014) occurred between the image dates, although two events were close (1 October 2010 at 148 m³/s and 11 April 2011 at 143 m³/s). It is clear from the 2011 images (Figures 2 and S2) that geomorphic changes occurred that could only be ascribed to severe flooding and Irene was the only such event in that time period.

2.5. Estimating Watershed-Scale Sediment and Phosphorus Export

To contextualize our estimates from the six Irene-affected stream bank sites studied here in terms of watershed-scale sediment and TP dynamics, we compared our estimates to the following: (a) areal channel-change measurements conducted over a greater length of the main stem for the same time period (2008–2011) (Jordan, 2013) and (b) watershed-scale suspended sediment and TP flux data estimated using data collected during other studies (Hamshaw et al., 2018; Jordan, 2013).

Jordan (2013) measured changes in stream position from air photos between 2008 and 2011 along 26 km of the Mad River's main stem (inclusive of our six sites), using the same methods as our study. She found an areal change of $215 \times 10^3 \text{ m}^2$ of bank retreat but did not measure depth or attempt to estimate mass loss from bank erosion. We extended her estimates in this study by assuming a conservative, average bank height of 1 m (about half the typical height we measured at our sites and in a more extended UAS; Hamshaw et al., 2017) and our average measured bulk density. We also conservatively assumed TP eroded along this entire

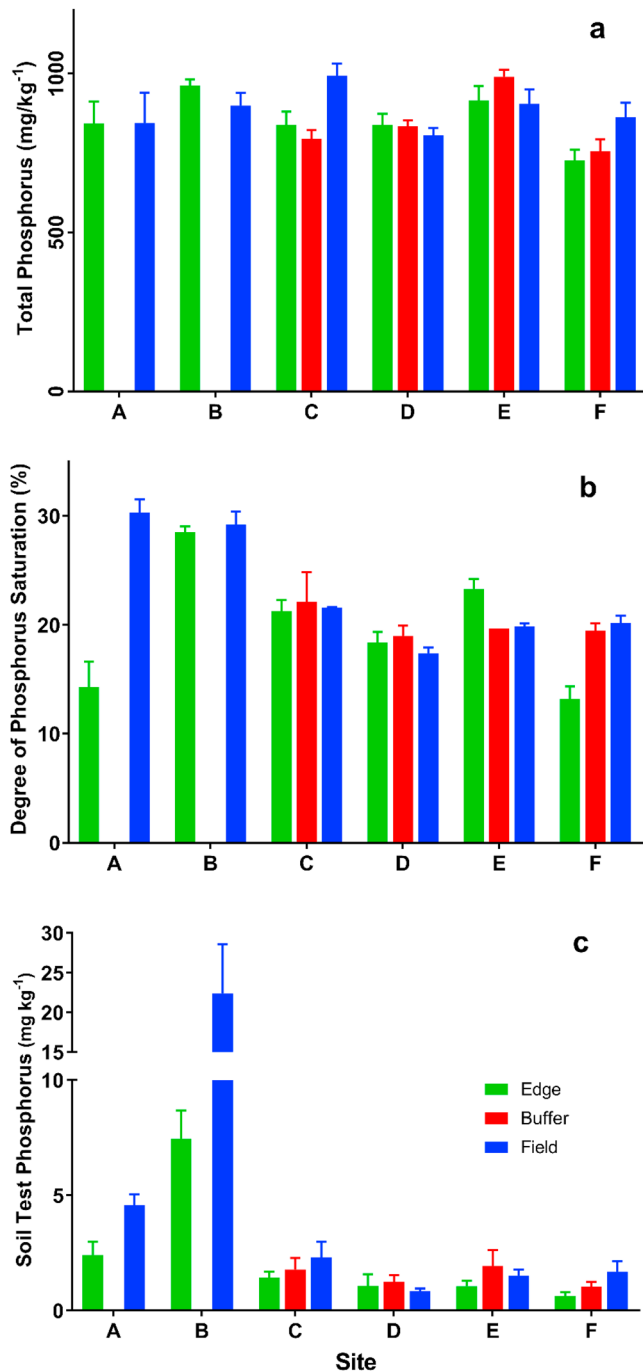


Figure 3. (a) Total phosphorus, (b) the degree of phosphorus saturation and (c) soil test (Modified Morgans) phosphorus in the 0- to 15-cm depth of the six sites. Error bars represent the standard error of the mean, which was taken from eight sampling points for each location (see Figure S1). Sites A and B had essentially no buffer.

length of the river corridor was equal to the low regional parent material average of 600 mg/kg (Yang et al., 2013).

We used two approaches to estimate watershed suspended sediment and TP export for time periods before, including, and after Irene. First, a rough estimate of watershed-scale total suspended solids (TSS) and TP export was derived through scaling of the average annual export of the larger Winooski watershed (Medalie, 2014) to that of the Mad River, which comprises 13.8% in the Winooski drainage area. The Winooski watershed estimates were calculated using daily mean discharge and a weighted regression with less frequent chemical analyses (monthly to bimonthly). We generated an annual average estimate based on 19 years of data prior to Irene and separately report Medalie's estimate for 2011, which includes the Irene flood event. Second, an estimate of average annual suspended sediment export was derived from data collected in a separate study by Hamshaw et al. (2018). TSS load from the Mad River watershed was estimated seasonally (early spring through late autumn) from 2013 to 2016 by surrogate monitoring using a turbidity sensor. To scale the seasonal TSS load estimates to the entire year, turbidity-based measurements from Hamshaw et al. (2018) were combined with estimates for the period when direct monitoring was not available (i.e., spring melt period) by referencing discharge data from the USGS stream gauge and utilizing existing regression relationships of TSS to discharge (Hamshaw, 2018). Average annual TSS export for the Mad River was then calculated using the cumulative TSS load from the four-year (2013 to 2016) period. Average annual TP export from the 2013–2016 period was similarly derived using a rating curve-based approach with power law regressions developed between turbidity and TP, and discharge and TP (Figure S3 and Table S1) from the turbidity and TP data collected by Hamshaw (2018). In both of the above cases, we related our site-specific erosion to watershed-scale export estimates by calculating the fraction of mass soil lost that would likely be transported during high flow events as suspended matter (as both silts and clays, and only clays).

3. Results

3.1. Soil Characterization

Stream corridor soils at our study sites were coarse in texture and relatively low in organic matter (Table 2). The soils were generally deep (i.e., >90 cm), with consistent textural class (sandy loams or loamy sands) throughout the profile (Table S2). At the two sites (C and E) where deeper samples were obtained, texture was again consistent with the upper profile. Gravel inclusions are not uncommon in these soils, and thin layers were found between 45 and 70 cm in profiles at Sites A and C.

The average TP in the 0- to 15-cm depth across transect locations (field, buffer, and stream bank edge) from the six stream bank sites ranged from 728 to 994 mg/kg and showed no clear trend along the transects (Figure 3a). There was also no clear trend in TP with depth (see data in the supporting information). The DPS was elevated in the hay field at

Site A and the hay field and stream bank edge in Site B (Figure 3b). Sites A and B were on active dairy and beef farms, respectively, and had minimal buffer zones in 2013 but obvious mixed vegetation buffers prior to Irene (Figure 2). STP was also elevated at these two locations, especially at Site B (4.6 and 22.4 mg/kg for the fields at Sites A and B respectively, Figure 3c). The optimum range for STP for crop growth in Vermont is 4–7 mg/kg, and anything above 20 mg/kg is considered excessive (Jokela et al., 2004). As

Table 3
Soil and Phosphorus Eroded Between 2008 and 2011, Including Calculation Parameters

Site	Length along stream (m)	Maximum width of eroded area (m)	Bank height (m)	Volume of soil eroded (m^{-3})	Mass of soil eroded (Mg)	Total phosphorus (mg/kg)	Total phosphorus eroded (kg)
A	158	11.6	2.4 ± 0.03	2677 ± 73	3743 ± 108	1066 ± 42	3990 ± 120
B	228	17.1	2.5 ± 0.24	3259 ± 778	4652 ± 1137	906 ± 52	4215 ± 1090
C	152	12.1	2.0 ± 0.14	1864 ± 258	2398 ± 345	836 ± 68	2006 ± 312
D	92	3.7	2.1 ± 0.05	293 ± 14	341 ± 16	858 ± 13	292 ± 14
E	112	32.9	1.7 ± 0.08	3603 ± 303	4780 ± 425	895 ± 38	4276 ± 397
F	120	9.3	2.0 ± 0.11	1306 ± 140	1665 ± 184	622 ± 54	1036 ± 124

Note. Error was calculated as the 95% confidence interval for all variables except total phosphorus, which uses the range of the duplicates. The error was propagated throughout the calculations.

would be expected, there was a clear decline in STP with depth at all locations to an average of 0.8 (SE 0.1) mg/kg in the 60- to 90-cm depth (data in the supporting information).

3.2. Stream bank Erosion

All of the sites we studied experienced channel changes between 2008 and 2011 (Table 3). The measured length of erosion along the stream bank at each site ranged from 92 to 228 m, with the maximum width of eroded area varying between 3.7 and 32.9 m. Bank heights ranged from 1.7 to 2.5 m and were relatively uniform within a given site, although Site B had a 1-m variation along its length. Soil bulk density also had a narrow range between 1.20 and 1.40 Mg/m^3 .

Estimated erosion mass varied from a high of 4,780 Mg (42.7 Mg/m of stream bank) at Site E to a low of 341 Mg (3.7 Mg/m) at Site D (Table 3). The mass of eroded soil per meter length of stream bank was well correlated with the maximum width of erosion. Estimated TP loss ranged from 292 kg (3.2 kg/m of stream bank) at Site D to 4,276 kg (38.2 kg/m) at Site E, where total erosion was also highest. These six sites together represented 0.87 km of stream bank and contributed 17.6×10^3 Mg of eroded soil containing 15.8 Mg of TP (20.4×10^3 Mg/km of soil and 18.4 Mg/km of TP). The bioavailable form of P, estimated with STP, was 2–3 orders of magnitude lower than TP. The depth-prorated concentration of STP in the near-stream soils varied from 0.3 mg/kg at Site F to 3.0 mg/kg at Site B compared to 622 mg/kg and 906 mg/kg, respectively, for the prorated TP concentrations. This translates to a total of 0.6 and 14.0 kg of STP eroded from these two sites, respectively.

The majority of the 17.6×10^3 Mg of eroded soil was sand sized (64–84%), and these coarser-grained sediments were likely not fully exported from the watershed due to in-stream (and possibly overbank) deposition. We calculated the fine fractions of the eroded soil at 4.8×10^3 Mg for the silt- and clay-sized particles and similarly 1.0×10^3 Mg for only the clay-sized particles (Table 4). These values are more appropriate for comparing our stream bank loss estimates to watershed-scale suspended sediment and TP exports (explored further in the following section).

3.3. Comparisons With Estimates of Main Stem Erosion and Watershed-Scale Annual Export

The main stem of the Mad River is ~35 km in length, and we estimated erosion losses from only 2.5% of this length, although we targeted high-eroding segments. Additionally, our transects were located on a single side of the river, not both. Using the erosional estimates of Jordan (2013) along 26 km of the main stem, and with our conservative use of an average bank height of 1 m, we calculated 274×10^3 Mg of stream bank erosion over the 3-year period that included Irene (Table 4). Most of this erosion was likely attributed to Irene and is about 15 times the erosion estimated from only our six sites (totaling 0.87 km of main stem). Similarly, using the erosion data from Jordan (2013), we estimated 165 Mg of TP contributed from stream banks along the main stem over the Irene period. The 0.87 km of eroded stream bank in this study contributed 15.8 Mg of TP in all size fractions (Table 4). Assuming the silt- and clay-sized particles had 1.3 times the TP of the bulk soil (a relationship between silt loam and loamy sand found in Ishee et al., 2015), the silt and clay fraction together would have 5.7 Mg of TP and the clay alone 1.2 Mg (Table 4).

Table 4
Estimates of Sediment Erosion and Export

Source of estimate	Portion of watershed	Time frame	Date	Sediment (Mg × 10 ³)	TP (Mg)
Erosion estimates					
This study—sum of the six sites	0.87 km of main stem	Irene period	Aug 2008 to Sep 2011	17.6	15.8
This study—sum of the six sites using only the clay- and silt-sized fraction	0.87 km of main stem	Irene period	Aug 2008 to Sep 2011	4.8	5.7
This study—sum of the six sites using only the clay-sized fraction	0.87 km of main stem	Irene period	Aug 2008 to Sep 2011	1.0	1.2
Jordan (2013)	26 km of main stem	Irene period	Aug 2008 to Sep 2011	274	165
Suspended export estimates					
Proportional ^a estimate using data from the larger Winooski River watershed (Medalie, 2014)	Entire	Annual average	1992–2010	16.1	22.5
Proportional ^a estimate using data from the larger Winooski River watershed (Medalie, 2014)	Entire	1 year (Irene)	2011	64.7	63.6
Mad River estimate using TSS, TP, turbidity, and discharge rating curves ^b (Hamshaw, 2018)	Above USGS gauge ^c	Annual average	2013–2016	28.3	15.8

Note. TSS = total suspended solids; TP = total phosphorus; USGS = United States Geological Survey.

^aYield estimate for Winooski River scaled to proportion of Winooski watershed comprising the Mad River (13.8%). ^bEstimates from 2013 to 2016 include the post-Irene period, characterized by near-normal mean annual flows, and a maximum peak flow of 222 m³/s (between a 2- to 5-year RI) on 15 April 2014. It also encompassed a 4 July 2013 flood event when a peak flow of 189 m³/s was recorded at the USGS gauge, resulting in inundation extents in the upper portion of the watershed (including at Sites D, E, and F). ^cThe watershed area above the USGS gauge is 92% of the total watershed area, but no major tributaries enter the river below it.

Erosion from our six stream bank sites produced estimated fluxes of sediment and TP during a single extreme event that were comparable to the calculated average annual fluxes derived from others (Table 4). Our estimates of suspended sediment export of the Mad River gave an annual average of 16.1×10^3 and 28.3×10^3 Mg of TSS export, from the Winooski-scaled and turbidity monitoring estimates, respectively. These estimates are both similar in magnitude to our 17.6×10^3 Mg of stream bank erosion (Table 4). The annual suspended sediment export from the Winooski for 2011, the year of Irene, was 4 times higher than the average of the prior 19 years (Medalie, 2014).

Similar to sediment, our calculations suggest that TP loading from Irene from just the six sites was comparable in magnitude to the long-term annual export averages (Table 4). The Mad River annual average TP export was 22.5 Mg of TP based on the Winooski-scale estimates and 15.8 Mg using the direct turbidity monitoring-based estimates. Annual TP loss during 2011 (Irene year) was estimated at 63.6 Mg, and nearly 4 times higher than annual average export during years not including Irene, consistent with results for TSS.

4. Discussion

The August 2011 flood in the Mad River valley during Tropical Storm Irene was an extreme event (200- to 500-year RI) that resulted in significant stream bank erosion driven by channel widening and meander migration, including at our six study sites located along the midwatershed reaches of the main stem (Figure 1). Bank erosion at these six main stem sites during the 2-day event generated mass inputs to the channel of fine sediments and TP that were similar in magnitude to average fluxes from the entire watershed over a typical year.

4.1. Geomorphic Context for Erosion Estimates

The magnitude of channel-floodplain change and its spatial distribution in response to an extreme event is a complex, nonlinear manifestation of several factors (Costa & O'Connor, 1995; Wolman & Gerson, 1978), including not only the magnitude, frequency, and duration of the event (Magilligan et al., 2015), antecedent conditions (Hooke, 2015), and channel characteristics (Buraas et al., 2014) but also the basin lithology and geomorphic setting (Costa & O'Connor, 1995). Valley confinement has been identified as a controlling factor in geomorphic effectiveness of extreme events, where lower-gradient, unconfined reaches have been characterized by more depositional conditions (Thompson & Croke, 2013) and enhanced planimetric adjustment (Righini et al., 2017), relative to confined reaches.

In our study, geomorphic assessments completed prior to Irene determined the reaches containing Sites B through F to be dominated by widening and aggradation processes (<https://anrweb.vt.gov/DEC/SGA/Default.aspx>, last accessed June 2018; reach containing Site A was not assessed). Sites A through E were located along channel reaches of relatively low gradient ($<0.5\%$) in unconfined valley settings (valley width/channel width > 14). The channel in each case is somewhat incised below the floodplain, based on cross sections completed after Irene proximal to our stream bank monitoring sites. According to a post-Irene one-dimensional Hydrologic Engineering Center-River Analysis System model (Dubois and King Inc., 2017), the 2.33-year RI flood is contained within the channel banks at Sites A through E. However, the modeled peak Irene stage inundated the floodplain at each site. The transect at Site F (Figure S2), in contrast, was located at a bedrock-controlled valley pinch point in an otherwise narrow to broad reach (valley width/channel width = 6.3). Modeled flows up to and exceeding the peak stage of the Irene flood were contained within the channel/valley banks at Site F. The erosion polygon examined at this site, however, extended upstream from the transect into a setting that is locally unconfined by valley walls. Irene floodwaters inundated this localized pocket of floodplain, located approximately 100 m upstream of Transect F.

None of our estimates of sediment input have included contributions from steeper tributaries. Based on limited field observations and anecdotal accounts, we note that significant erosion and deposition occurred along tributary reaches during Irene. These steeper-gradient reaches tend to be more closely coupled to hillslopes comprised of glacial till, and to glaciolacustrine and glaciofluvial terraces (Dunn et al., 2007), that are subject to mass wasting (Springston, 2017). It is possible that sediment sourced from these headwaters led to coarse sediment aggradation along the main stem and contributed to channel widening and planform adjustment at our six study sites. Additionally, fine sediment ($<63 \mu\text{m}$) sourced from the steeper tributaries likely contributed to watershed-scale export of TSS (and possibly TP). Our study does not convey a full accounting of the Irene event sediment budget for the watershed, nor does it represent a comprehensive examination of hydraulic or geomorphic variables with the potential to control channel and floodplain response to this extreme event. Rather, our research represents a case study of stream bank erosion resulting from an extreme event and demonstrates the utility of aerial surveys paired with transect sampling to generate estimates of sediment and TP loss due to channel adjustment.

4.2. Potential Limitations of Measurements and Estimates

As stated above, our erosion measurements are likely high estimates for watershed sediment export. We did not account for stream bed retention or attenuation of suspended sediments in overbank areas of the floodplain, or behind impoundments. However, sediment deposited in the stream bed will likely contribute to export in subsequent events and most will eventually be exported. Our two full-watershed export estimates differed, and this could partially be attributed to the impact of impoundments downstream of the USGS gauge on the Mad River and along the Winooski as well as the Winooski-based estimates being pre-Irene and Mad River estimates being post-Irene. While both estimates have different limitations, our intent was to highlight the effect of one extreme event relative to annual norms rather than accurately quantify watershed sediment and P export.

We assumed that the stream bank heights measured after Irene (2016 UAS) were similar to those that existed before Irene. Given that the study areas were relatively closely spaced along the valley floor (resulting in a relatively low range in upstream drainage area) and had low variability in current bank heights among the sites suggests that this may be the case, but there are no available data to unequivocally demonstrate this. For calculating the mass of soil and TP loss, we also assumed that the current near-stream soils were the same in character as the soil eroded. Again, there was low variability in both particle size and texture across the sites, and this assumption appears reasonable. The assumption that the soil deeper than 90 cm had the same TP as the 60- to 90-cm layer appeared to be reasonable at the two sites with deeper samples. Site B had an average concentration in the 60- to 90-cm depth of 805 mg/kg and one sample each from 90–120 and 120–150 cm with TP of 801 and 761 mg/kg, respectively (Data Set S1 in the supporting information). Site E had one deeper sample taken, 90–120 cm, which had 878 mg/kg (Data Set S1), whereas the 60- to 90-cm samples had an average of 874 mg/kg. Finally, we used soil bulk density measurements from the surface 0–15 cm for the full soil loss profile, and we did not include any estimates of coarse fragments, in either the mass or TP calculations. These two assumptions should more or less cancel each other out as the subsurface soils are usually denser than the surface (due to lower organic matter), but the actual mass of soil will be lower if coarse

fragments (>2 mm) are excluded. Ishee et al. (2015), working with near-stream soils in another part of the Winooski watershed, found about a 20% increase in bulk density in soils 25–150 cm deep compared to 0–15 cm. A firm estimate of coarse fragments is not available because we did not sample to the depth of the stream banks (and obviously did not sample the already eroded stream bank soils). However, Sites A, C, and E had USDA NRCS characterization pits located within 10 m of the transects and excavated to depths of 130, 140, and 147 cm, respectively (S2013VT023001, –2, and –3; Soil Survey Staff, 2017b). The pits at Sites C and E averaged <1% coarse fragments down to 140+ cm, with Site E having a gravelly layer from 144 to 147 (57% coarse fragments). Site A had more gravel throughout the profile, averaging 3% in the top 55 cm and 21% in the bottom 75 cm.

4.3. Total and Bioavailable Phosphorus Relative to Other Studies

The mean TP at all six of our sites was above the mean of 621 ± 21 mg/kg found by Ishee et al. (2015) in similar depth sampling of near-stream soils in Lake Champlain tributaries further west of the Mad River. Other studies of near-stream soils in Vermont have found similarly low average concentrations (DeWolfe et al., 2004; Young et al., 2012). The average concentration in soils across the United States (Abrams & Jarrell, 1995) and the regional concentration in parent material (Yang et al., 2013) is 600 mg/kg. Soils with a history of agricultural land use can have “legacy” P (Sharpley et al., 2013), and near-stream soils can be elevated depending on the presence or absence of an effective riparian buffer. Near-stream soils associated with agricultural land use have been elevated in other areas of the Basin, as high as 1,874 mg/kg TP (Young et al., 2012). The trend in TP in our study (Table 3) was higher in the sites with active agriculture (A and B) and elevated STP and DPS. Because we sampled after Irene, it is possible that the stream banks eroded during Irene at these two sites had somewhat lower (e.g., 20–30%) TP, more similar to the mean found at other sites. The near-stream soils sampled in this study post Irene may have been high in P due to their former, more interior position where they could have received additions of manure and/or fertilizer. If so, our estimates of TP erosional loss could be somewhat inflated.

Loss of bioavailable P, as estimated by STP, was a small percentage of the overall TP export. Much of the eroded soil, especially below the 0- to 15-cm layer, was quite low in both STP and DPS, suggesting relatively low release of dissolved P. Similar results were found by Ishee et al. (2015) in the western portion of the Winooski watershed in tributaries with mixed land use but low agriculture. Assuming the eroded stream banks in our study had similar STP to what we measured and it all dissolved from the eroded soil into the stream and was exported to Lake Champlain without undergoing subsequent transformation, the total bioavailable P export would be 0.04 Mg. This total can be compared to the annual average export of dissolved P (<0.45 μm), normalized to the Mad River from the larger Winooski (Medalie, 2014), which was 2.8 Mg from 1992 to 2010. However, such a simple comparison does not account for the complexities of instream nutrient cycling that would undoubtedly occur along the Mad River and lower Winooski River. For example, Grundtner et al. (2014) showed that sediment from eroded stream banks in Minnesota likely sorbed dissolved P during transport and deposition downstream. The stream bank sediments eroded into the Mad River could potentially be a temporary sink for dissolved P, but any P sorbed by Fe oxides could also be released if the sediments become anoxic (Young & Ross, 2001). There are dams at select locations along the Mad River and Winooski River main stems with potential for transient storage of sediments in the resulting impoundments. Anoxic conditions can occur in shallow sediments of these impoundments or in the ultimate receiving waters of Lake Champlain where such conditions have been linked to algal blooms (Isles et al., 2015, 2017).

During Irene, additional inputs of bioavailable P to the stream could have resulted from greatly increased overland flow and surface runoff. However, monitoring in other watersheds along the path of Irene showed that particulate forms of P increased much more than dissolved forms (Vidon et al., 2018). The influx of particulate P appeared to far exceed wash of bioavailable P.

4.4. Local and Regional Impacts

The effects of Tropical Storm Irene will likely influence stream bank erosion for the foreseeable future. Continued unusually high suspended sediment concentrations have been reported post Irene in streams of the Connecticut watershed (Yellen et al., 2014). One important impact of the extreme event was the extent of stream bank loss, usually extending beyond established vegetated riparian buffers. As can be seen from the images (Figures 2 and S2), many of the fields had narrow strips of large trees along the stream bank

that were removed during the event. These narrow buffers were easily stripped, particularly as incised and entrenched channels experienced enhanced stream power leading to fluvial erosion. Tree buffers are now absent along the newly eroded stream banks, and, in the case of Site B (managed cropland), the current stream bank has elevated STP and DPS (relative to the other sites). The new stream edge is located where the field was formerly cropped. Stream bank failure has continued at most of our study sites. Shortly before soil sampling, ~6 m of bank was lost from Site E during a flood event on 3–4 July 2013 (Anderson et al., 2013). Once eroded, coarse stream bank sediment could be deposited in downstream reaches and become a driver for bank retreat in future high flows. Continued higher rates of stream bank loss will also increase the likelihood of proportionally greater bioavailable P transport as the stream channel moves into soils previously amended with P in fertilizer and manure (legacy P). The loss of the wooded riparian buffers will have long-lasting effects on stream bank stability especially in light of time needed to reestablish mature trees, and the limitations on buffer width imposed by adjacent agricultural or developed land uses.

With projected increases in both the quantity of precipitation (Huang et al., 2018; Intergovernmental Panel on Climate Change, 2013) and the frequency of extreme events (Horton & Liu, 2014) due to climate change, the rivers of the northeastern United States will likely continue to experience unprecedented discharge and cascading downstream effects (Vidon et al., 2018) such as those apparent during Tropical Storm Irene. The Mad River watershed (Figure 1) comprises a relatively small area of the Lake Champlain basin, but similar extreme flows were observed throughout the upper Winooski River sub-basin (Olson, 2015). Sediment (TSS) discharge at the mouth of the Winooski for 29 August 2011 (the day after Irene entered Vermont) was 126×10^3 Mg, which is higher than the average annual export from 1992 to 2012 (excluding 2011) of 113×10^3 Mg (Medalie, 2014). Similar high sediment discharges were seen in two of the major watersheds of the northeastern United States—the Hudson and Connecticut Rivers. Ralston et al. (2013) found that the combined effects of Tropical Storms Irene and Lee (which closely followed Irene) delivered about 5 times the normal annual input of sediment to the Hudson River. Sediment load in the lower Connecticut River over the 3 days of peak flow due to Tropical Storm Irene was about twice the average annual load (Yellen et al., 2014). The source of this sediment was both from channel widening, or typical stream bank erosion, and stream-adjacent mass wasting (Dethier et al., 2016). Region-wide impacts from stream bank erosion would likely have been more severe if the extreme event had a longer duration. Magilligan et al. (2015) observed that channel widening in Saxton's River in southeastern Vermont (Connecticut River watershed) was less than expected because of the short duration of sufficient stream power (~6 hr). New channel avulsion and mass wasting mobilized sediments likely not exposed since glaciation (Magilligan et al., 2015; Yellen et al., 2016). It is possible that similar upland sediments contributed to export from the Mad River during Irene. This sediment would not contain legacy P from agriculture and, similar to most of the soils we sampled, would not be expected to immediately contribute bioavailable P downstream. Regardless of the exact source, it is evident that extreme precipitation events, such as Tropical Storm Irene, can have regional impacts on sediment movement.

5. Conclusions

This case study details geomorphic effectiveness of a relatively short duration, extreme precipitation event on six discrete sites along the main stem of a small, mountainous New England river. Extensive stream bank retreat, sediment, and P loss occurred. The availability of timely, high-resolution aerial imagery offered an effective method to measure channel movement at highly vulnerable sites. We estimated that the load of sediment and P from <1 km of stream bank during this one event was similar in magnitude to the long-term average annual export. High post-Irene rates of stream bank erosion and sediment transport are likely due, in part, to instability caused by this event (Dethier et al., 2016). Continued high rates of erosion are probable given the projected increased likelihood of recurring extreme precipitation events (Hayhoe et al., 2007). The Irene-induced contribution of immediately bioavailable P appeared to be relatively low, but continued erosion will contribute sediment with higher concentrations of legacy P. Our study contributes to a body of literature on these geomorphically and biogeochemically important rare events and underscores the importance of extreme storms in sediment and nutrient flux from mountainous watersheds. Given the long recovery times from extreme events in humid temperate regions (Wolman & Gerson, 1978), these effects will be long-lasting.

Traditionally, management recommendations for agricultural lands consider rivers to be static in planform with a prescribed set back from the stream bank for agricultural activities and minimum widths of riparian buffers. In reality, rivers are very dynamic, and extreme events, particularly in unconfined settings, can drive substantial channel widening and wholesale removal of buffers. In the process, inland field areas more concentrated in particulate and bioavailable forms of P become accessible to stream bank erosion, raising the possibility that increased sediment and nutrient loading may be a persistent legacy of these extreme events. To mitigate for nutrient and sediment loading in a future where extreme events are projected to increase in magnitude and frequency (Guilbert et al., 2014), greater protective measures may be warranted including increased riparian buffer widths, improved nutrient management, and alternate cropping and grazing practices to reduce nutrient inputs.

Acknowledgments

The data used in this study are included in the supporting information. Donald Ross and Beverley Wemple's efforts were supported by the National Science Foundation under VT EPSCoR Grant Nos EPS-1101317 and NSF OIA 1556770. We would like to thank undergraduate interns Maria Diaz, Patrick Murphy, Elizabeth Olliver, Paloma Rodriguez, and Emily Secor, all supported by VT EPSCoR's Center for Workforce Development and Diversity under the first grant listed above (Lindsay Willson's efforts were also supported by this grant). Thanks to Joel Tilley for laboratory support and Caroline Alves, formerly of the USDA NRCS, for coordinating soil pit locations. We also gratefully acknowledge contributions from Mandar Dewoolkar and Donna Rizzo to various elements of this study. In addition, we would like to thank the landowners at each site for giving site access and permission to sample. Any opinions, findings, and conclusions or recommendations expressed in this material are those of the author(s) and do not necessarily reflect the views of the National Science Foundation.

References

- Abernethy, B., & Rutherford, I. D. (2000). The effect of riparian tree roots on the mass-stability of riverbanks. *Earth Surface Processes and Landforms*, 25(9), 921–937. [https://doi.org/10.1002/1096-9837\(200008\)25:9<921::AID-ESP93>3.0.CO;2-7](https://doi.org/10.1002/1096-9837(200008)25:9<921::AID-ESP93>3.0.CO;2-7)
- Abrams, M. M., & Jarrell, W. M. (1995). Soil phosphorus as a potential nonpoint source for elevated stream phosphorus levels. *Journal of Environmental Quality*, 24(1), 132–138. <https://doi.org/10.2134/jeq1995.00472425002400010019x>
- Anderson, D. M., Gibert, P. M., & Burkholder, J. M. (2002). Harmful algal blooms and eutrophication: Nutrient sources, composition, and consequences. *Estuaries*, 25(4), 704–726. <https://doi.org/10.1007/bf02804901>
- Anderson, H., Hamshaw S. D., Underwood K. L., Dewoolkar M. M., & Rizzo D. (2013). Estimates of sediment loading from streambank erosion using terrestrial LiDAR. Paper presented at 2013 Fall Meeting, AGU, San Francisco, CA, 9–13 Dec.
- Anderson, I., Rizzo, D. M., Huston, D. R., & Dewoolkar, M. M. (2017). Analysis of bridge and stream conditions of over 300 Vermont bridges damaged in Tropical Storm Irene. *Structure and Infrastructure Engineering*, 13(11), 1437–1450. <https://doi.org/10.1080/15732479.2017.1285329>
- Buraas, E. M., Renshaw, C. E., Magilligan, F. J., & Dade, W. B. (2014). Impact of reach geometry on stream channel sensitivity to extreme floods. *Earth Surface Processes and Landforms*, 39(13), 1778–1789. <https://doi.org/10.1002/esp.3562>
- Bussi, G., Francés, F., Horel, E., López-Tarazón, J. A., & Batalla, R. J. (2014). Modelling the impact of climate change on sediment yield in a highly erodible Mediterranean catchment. *Journal of Soils and Sediments*, 14(12), 1921–1937. <https://doi.org/10.1007/s11368-014-0956-7>
- Carpenter, S. R., Caraco, N. F., Correll, D. L., Howarth, R. W., Sharpley, A. N., & Smith, V. H. (1998). Nonpoint pollution of surface waters with phosphorus and nitrogen. *Ecological Applications*, 8(3), 559–568. [https://doi.org/10.1890/1051-0761\(1998\)008\[0559:NPOSWW\]2.0.CO;2](https://doi.org/10.1890/1051-0761(1998)008[0559:NPOSWW]2.0.CO;2)
- Costa, J. E., & O'Connor, J. E. (1995). Geomorphically effective floods. In J. E. Costa, A. J. Miller, K. W. Potter, & P. Wilcock (Eds.), *Natural and anthropogenic influences in fluvial geomorphology* (pp. 45–56). Washington, DC: American Geophysical Union. <https://doi.org/10.1029/GM089p0045>
- Courchesne, F., & Turmel, M.-C. (2007). Extractable Al, Fe, Mn and Si. In M. R. Carter & E. G. Gregorich (Eds.), *Soil sampling and methods of analysis* (pp. 307–315). Boca Raton, FL: CRC Press.
- Day, P. R. (1965). Particle fractionation and particle size analysis. In C. A. Black (Ed.), *Methods of soil analysis, part 1* (pp. 545–567). Madison, WI: American Society of Agronomy.
- Death, R. G., Fuller, I. C., & Macklin, M. G. (2015). Resetting the river template: The potential for climate-related extreme floods to transform river geomorphology and ecology. *Freshwater Biology*, 60(12), 2477–2496. <https://doi.org/10.1111/fwb.12639>
- Dethier, E., Magilligan, F. J., Renshaw, C. E., & Nislow, K. H. (2016). The role of chronic and episodic disturbances on channel-hillslope coupling: The persistence and legacy of extreme floods. *Earth Surface Processes and Landforms*, 41(10), 1437–1447. <https://doi.org/10.1002/esp.3958>
- DeWolfe, M. N., Hession, W. C., & Watzin, M. C. (2004). Sediment and phosphorus loads from streambank erosion in Vermont, USA. In G. Sehlke, D. F. Hayes, & D. K. Stevens (Eds.), *Critical Transactions in Water and Environmental Resources Management* (pp. 1–10). Reston, VA: American Society of Civil Engineers.
- Dubois and King Inc. (2017). Flood study: Mad River area: Towns of Fayston, Moretown, Waitsfield, Warren and Waterbury, Washington County, Vermont, prepared for Central Vermont Regional Planning Commission. Retrieved from <http://centralvtplanning.org/>
- Dunn, R., Springston G., & Donahue N. (2007). Surficial geologic map of the Mad River watershed, Vermont VGS Open-File Report VG07-1. Retrieved from <http://dec.vermont.gov/sites/dec/files/geo/OpenFile/VG071MadRiverSurfN.pdf>, <http://dec.vermont.gov/sites/dec/files/geo/OpenFile/VG071BMadRiverSurfS.pdf>
- Environmental Systems Research Institute (2017). ArcGIS Desktop 10.5.1, Environmental Systems Research Institute, Redlands, CA.
- Fox, G. A., Purvis, R. A., & Penn, C. J. (2016). Streambanks: A net source of sediment and phosphorus to streams and rivers. *Journal of Environmental Management*, 181, 602–614. <https://doi.org/10.1016/j.jenvman.2016.06.071>
- Gonzalez-Hidalgo, J. C., Batalla, R. J., Cerdà, A., & de Luis, M. (2010). Contribution of the largest events to suspended sediment transport across the USA. *Land Degradation & Development*, 21(2), 83–91. <https://doi.org/10.1002/ldr.897>
- Grundtner, A., Gupta, S., & Bloom, P. (2014). River bank materials as a source and as carriers of phosphorus to Lake Pepin. *Journal of Environmental Quality*, 43(6), 1991–2001. <https://doi.org/10.2134/jeq2014.03.0131>
- Guilbert, J., Beckage, B., Winter, J. M., Horton, R. M., Perkins, T., & Bombliès, A. (2014). Impacts of projected climate change over the Lake Champlain Basin in Vermont. *Journal of Applied Meteorology and Climatology*, 53(8), 1861–1875. <https://doi.org/10.1175/jamc-d-13-0338.1>
- Hamshaw, S. D. (2018). *Fluvial processes in motion: Measuring bank erosion and suspended sediment flux using advanced geomatics and machine learning*. Burlington, VT: University of Vermont.
- Hamshaw, S. D., Bryce, T., Rizzo, D. M., O'Neil-Dunne, J., Frolik, J., & Dewoolkar, M. M. (2017). Quantifying streambank movement and topography using unmanned aircraft system photogrammetry with comparison to terrestrial laser scanning. *River Research and Applications*, 33(8), 1354–1367. <https://doi.org/10.1002/rra.3183>
- Hamshaw, S. D., Dewoolkar, M. M., Schroth, A. W., Wemple, B. C., & Rizzo, D. M. (2018). A new machine-learning approach for classifying hysteresis in suspended-sediment discharge relationships using high-frequency monitoring data. *Water Resources Research*, 54, 4040–4058. <https://doi.org/10.1029/2017WR022238>
- Hayhoe, K., Wake, C. P., Huntington, T. G., Luo, L., Schwartz, M. D., Sheffield, J., et al. (2007). Past and future changes in climate and hydrological indicators in the US Northeast. *Climate Dynamics*, 28(4), 381–407. <https://doi.org/10.1007/s00382-006-0187-8>

- Hooke, J. M. (2015). Variations in flood magnitude–effect relations and the implications for flood risk assessment and river management. *Geomorphology*, 251, 91–107. <https://doi.org/10.1016/j.geomorph.2015.05.014>
- Horton, R. M., & Liu, J. (2014). Beyond Hurricane Sandy: What might the future hold for tropical cyclones in the North Atlantic? *Journal of Extreme Events*, 01(01), 1450007. <https://doi.org/10.1142/s2345737614500079>
- Huang, H., Winter, J. M., & Osterberg, E. C. (2018). Mechanisms of abrupt extreme precipitation change over the Northeastern United States. *Journal of Geophysical Research: Atmospheres*, 123, 7179–7192. <https://doi.org/10.1029/2017JD028136>
- Intergovernmental Panel on Climate Change (2013). Climate change 2013: The physical science basis In T. F. Stocker et al. (Eds.), *Contribution of Working Group I to the Fifth Assessment Report of the Intergovernmental Panel on Climate Change* (p. 1535). Cambridge, UK and New York: Cambridge University Press. <https://doi.org/10.1017/CBO9781107415324>
- Ishee, E. R., Ross, D. S., Garvey, K. M., Bourgault, R. R., & Ford, C. R. (2015). Phosphorus characterization and contribution from eroding streambank soils of Vermont's Lake Champlain Basin. *Journal of Environmental Quality*, 44(6), 1745–1753. <https://doi.org/10.2134/jeq2015.02.0108>
- Isles, P. D. F., Giles, C. D., Gearhart, T. A., Xu, Y., Druschel, G. K., & Schroth, A. W. (2015). Dynamic internal drivers of a historically severe cyanobacteria bloom in Lake Champlain revealed through comprehensive monitoring. *Journal of Great Lakes Research*, 41(3), 818–829. <https://doi.org/10.1016/j.jglr.2015.06.006>
- Isles, P. D. F., Xu, Y., Stockwell, J. D., & Schroth, A. W. (2017). Climate-driven changes in energy and mass inputs systematically alter nutrient concentration and stoichiometry in deep and shallow regions of Lake Champlain. *Biogeochemistry*, 133(2), 201–217. <https://doi.org/10.1007/s10533-017-0327-8>
- Jokela, W., Magdoff, F., Bartlett, R., Bosworth S., & Ross, D. (2004). Nutrient recommendations for field crops in Vermont (Extension Bulletin Br. 1390 1390, 27 pp.). Burlington, VT.
- Jordan, L. (2013). Stream Channel Migration of the Mad River between 1995 and 2011 (48 pp.). University of Vermont.
- Kronvang, B., Audet, J., Baattrup-Pedersen, A., Jensen, H. S., & Larsen, S. E. (2012). Phosphorus load to surface water from bank erosion in a Danish lowland river basin. *Journal of Environmental Quality*, 41(2), 304–313. <https://doi.org/10.2134/jeq2010.0434>
- Langendoen, E. J., Simon A., Klimetz L., Bankhead N., & Ursic M. E. (2012). Quantifying sediment loadings from streambank erosion in selected agricultural watersheds draining to Lake Champlain, (Lake Champlain Basin Program Technical Report No. 72, 65 pp.). Burlington, VT.
- Leytem, A. B., & Kpombekou-A, K. (2009). Total phosphorus in soil. In J. L. Kovar & G. M. Pierzynski (Eds.), *Methods of phosphorus analysis for soils, sediments residuals, and waters* (pp. 44–50). Blacksburg, VA: Virginia Tech University
- Magdoff, F. R., Hryshko, C., Jokela, W. E., Durieux, R. P., & Bu, Y. (1999). Comparison of phosphorus soil test extractants for plant availability and environmental assessment. *Soil Science Society of America Journal*, 63(4), 999–1006. <https://doi.org/10.2136/sssaj1999.634999x>
- Magilligan, F. J., Buraas, E. M., & Renshaw, C. E. (2015). The efficacy of stream power and flow duration on geomorphic responses to catastrophic flooding. *Geomorphology*, 228, 175–188. <https://doi.org/10.1016/j.geomorph.2014.08.016>
- Medalie, L. (2014). Concentration and flux of total and dissolved phosphorus, total nitrogen, chloride, and total suspended solids for monitored tributaries of Lake Champlain, 1990–2012, (U.S. Geological Survey Scientific Investigations Report 2014-1209, 21 pp.). <https://doi.org/10.3133/ofr20141209>
- Merritt, D. M. (2013). Reciprocal relations between riparian vegetation, fluvial landforms, and channel processes. In E. Wohl (Ed.), *Treatise on geomorphology* (pp. 219–243). Amsterdam: Elsevier. <https://doi.org/10.1016/B978-0-12-374739-6.00239-6>
- Miller, R. B., Fox, G. A., Penn, C. J., Wilson, S., Parnell, A., Purvis, R. A., & Criswell, K. (2014). Estimating sediment and phosphorus loads from streambanks with and without riparian protection. *Agriculture, Ecosystems & Environment*, 189, 70–81. <https://doi.org/10.1016/j.agee.2014.03.016>
- Naylor, L. A., Spencer, T., Lane, S. N., Darby, S. E., Magilligan, F. J., Macklin, M. G., & Möller, I. (2017). Stormy geomorphology: Geomorphic contributions in an age of climate extremes. *Earth Surface Processes and Landforms*, 42(1), 166–190. <https://doi.org/10.1002/esp.4062>
- Nearing, M. A., Pruski, F. F., & O'Neill, M. R. (2004). Expected climate change impacts on soil erosion rates: A review. *Journal of Soil and Water Conservation*, 59, 43–50.
- Olson, S. A. (2014). Estimation of flood discharges at selected annual exceedance probabilities for unregulated, rural streams in Vermont, with a section on Vermont regional skew regression, by Veilleux, A.G., (U.S. Geological Survey Scientific Investigations Report 2014-5078, 27 pp.). <https://doi.org/10.3133/sir20145078>
- Olson, S. A. (2015). Flood maps for the Winooski River in Waterbury, Vermont, 2014, (U.S. Geological Survey Scientific Investigations Report 2015-5077, 25 pp.). <https://doi.org/10.3133/sir20155077>
- Osborne, L. L., & Kovacic, D. A. (1993). Riparian vegetated buffer strips in water-quality restoration and stream management. *Freshwater Biology*, 29(2), 243–258. <https://doi.org/10.1111/j.1365-2427.1993.tb00761.x>
- Ralston, D. K., Warner, J. C., Geyer, W. R., & Wall, G. R. (2013). Sediment transport due to extreme events: The Hudson River estuary after tropical storms Irene and Lee. *Geophysical Research Letters*, 40, 5451–5455. <https://doi.org/10.1002/2013GL057906>
- Righini, M., Surian, N., Wohl, E., Marchi, L., Comiti, F., Amponsah, W., & Borga, M. (2017). Geomorphic response to an extreme flood in two Mediterranean rivers (northeastern Sardinia, Italy): Analysis of controlling factors. *Geomorphology*, 290, 184–199. <https://doi.org/10.1016/j.geomorph.2017.04.014>
- Schulte, E. E., & Hoskins B. (2011). In D. Beegle & A. Wolf (Eds.), *Recommended soil testing procedures for the Northeastern United States, Northeast Region Publication No. 493*. Newark, DE.
- Sekely, A. C., Mulla, D. J., & Bauer, D. W. (2002). Streambank slumping and its contribution to the phosphorus and suspended sediment loads of the Blue Earth River, Minnesota. *Journal of Soil and Water Conservation*, 57(5), 243–250.
- Shanley, J. B., & Denner, J. C. (1999). The hydrology of the Lake Champlain Basin. In T. O. Manley & P. L. Manley (Eds.), *Lake Champlain in transition: From research toward restoration* (pp. 41–66). Washington, DC: American Geophysical Union. <https://doi.org/10.1029/WS001p0041>
- Sharpley, A., Jarvie, H. P., Buda, A., May, L., Spears, B., & Kleinman, P. (2013). Phosphorus legacy: Overcoming the effects of past management practices to mitigate future water quality impairment. *Journal of Environmental Quality*, 42(5), 1308–1326. <https://doi.org/10.2134/jeq2013.03.0098>
- Smeltzer, E., Shambaugh, A. d., & Stangel, P. (2012). Environmental change in Lake Champlain revealed by long-term monitoring. *Journal of Great Lakes Research*, 38, 6–18. <https://doi.org/10.1016/j.jglr.2012.01.002>
- Soil Survey Staff (2017a). Web soil survey, United States Department of Agriculture. Natural Resources Conservation Service. Retrieved from <https://websoilsurvey.sc.egov.usda.gov>

- Soil Survey Staff (2017b). Soil data mart, Natural Resources Conservation Service, United States Department of Agriculture. Retrieved from <https://ncsslabsdatamart.sc.egov.usda.gov>
- Springston, G. (2017). Landslide inventory of Washington County, central Vermont, Open File Report VG2017–VG2017. Retrieved from <http://dec.vermont.gov/sites/dec/files/geo/HazDocs/WashingtonCtyInstabilityRpt2017.pdf>
- Stryker, J., Wemple, B., & Bomblied, A. (2018). The impacts of climate change on sediment mobilization and transport. *Journal of Hydrology Regional Studies*, 17, 83–94. <https://doi.org/10.1016/j.ejrh.2018.04.003>
- Thompson, C., & Croke, J. (2013). Geomorphic effects, flood power, and channel competence of a catastrophic flood in confined and unconfined reaches of the upper Lockyer valley, southeast Queensland, Australia. *Geomorphology*, 197, 156–169. <https://doi.org/10.1016/j.geomorph.2013.05.006>
- Troy, A., Wang, D., Capen, D., O'Neil-Dunne, J., & MacFaden, S. (2007). Updating the Lake Champlain basin land use data to improve prediction of phosphorus loading, (Lake Champlain Basin Program Technical Report No. 54, 121 pp.). Grand Isle, VT. Retrieved from http://www.lcbp.org/wp-content/uploads/2013/04/54_LULC-Phosphorus_2007.pdf
- United States Environmental Protection Agency (2007). Microwave assisted acid digestion of sediments, sludges, soils, and oils, (United States Environmental Protection Agency SW-846, 30 pp.). Retrieved from <https://www.epa.gov/sites/production/files/2015-12/documents/3051a.pdf>
- Vidon, P., Karwan, D. L., Andres, A. S., Inamdar, S., Kaushal, S., Morrison, J., et al. (2018). In the path of the hurricane: Impact of Hurricane Irene and Tropical Storm Lee on watershed hydrology and biogeochemistry from North Carolina to Maine, USA. *Biogeochemistry*, 141(3), 351–364. <https://doi.org/10.1007/s10533-018-0423-4>
- Vidon, P., Marchese, S., & Rook, S. (2017). Impact of Hurricane Irene and Tropical Storm Lee on riparian zone hydrology and biogeochemistry. *Hydrological Processes*, 31(2), 476–488. <https://doi.org/10.1002/hyp.11045>
- Wolf, A., & Beegle, D. (2011). Recommended soil tests for macronutrients: Phosphorus, potassium, calcium, and magnesium, In D. Beegle, & A. Wolf (Eds.), *Recommended Soil Testing Procedures for the Northeastern United States, Northeast Region Publication No. 493*. Newark, DE.
- Wolman, M. G., & Gerson, R. (1978). Relative scales of time and effectiveness of climate in watershed geomorphology. *Earth Surface Processes and Landforms*, 3(2), 189–208. <https://doi.org/10.1002/esp.3290030207>
- Yang, X., Post, W. M., Thornton, P. E., & Jain, A. (2013). The distribution of soil phosphorus for global biogeochemical modeling. *Biogeosciences*, 10(4), 2525–2537. <https://doi.org/10.5194/bg-10-2525-2013>
- Yellen, B., Woodruff, J. D., Cook, T. L., & Newton, R. M. (2016). Historically unprecedented erosion from Tropical Storm Irene due to high antecedent precipitation. *Earth Surface Processes and Landforms*, 41(5), 677–684. <https://doi.org/10.1002/esp.3896>
- Yellen, B., Woodruff, J. D., Kratz, L. N., Mabee, S. B., Morrison, J., & Martini, A. M. (2014). Source, conveyance and fate of suspended sediments following Hurricane Irene. New England, USA. *Geomorphology*, 226, 124–134. <https://doi.org/10.1016/j.geomorph.2014.07.028>
- Young, E. O., & Ross, D. S. (2001). Phosphate release from seasonally flooded soils. *Journal of Environmental Quality*, 30(1), 91–101. <https://doi.org/10.2134/jeq2001.30191x>
- Young, E. O., Ross, D. S., Alves, C., & Villars, T. (2012). Soil and landscape influences on native riparian phosphorus availability in three Lake Champlain Basin stream corridors. *Journal of Soil and Water Conservation*, 67(1), 1–7. <https://doi.org/10.2489/jswc.67.1.1>
- Zaimes, G. N., Schultz, R. C., & Isenhardt, T. M. (2008). Streambank soil and phosphorus losses under different riparian land-uses in Iowa. *Journal of the American Water Resources Association*, 44(4), 935–947. <https://doi.org/10.1111/j.1752-1688.2008.00210.x>